Historical Weather Observations and Potential Future Climate Scenarios for Summit Lake, Nevada Region

Information for Summit Lake Paiute Tribe Climate Adaptation Plan

By

Sandra E. Yuter
Philip E. Zimmer
Matthew A. Miller
L. Baker Perry

The University of Nevada–Reno
and North Carolina State University

NC STATE
UNIVERSITY

Executive Summary

Weather observations over the last several decades as well as climate projections for the local area of Summit Lake and the regional area of northern Nevada surrounding Summit Lake were examined to inform climate adaptation planning by the Summit Lake Paiute Tribe. Data were organized by seasons (December-January-February, March-April-May, June-July-August, September-October-November). Analysis looked for trends and variability. Historical analysis over the period 1990-2023 is based on the largely complete daily records for temperature from 13 weather stations and for precipitation from 5 weather stations. Climate projections are based on data used by the United Nations Intergovernmental Panel on Climate Change.

Use of different input greenhouse gas emissions scenarios (the rate that the CO_2 concentration in the atmosphere changes per year) yield larger contrasts among future temperature predictions than differences in representing earth system physical processes among different modeling groups. This report uses climate predictions from a likely emissions scenario and a low probability worse case scenario.

Weather forecast and climate prediction models are generally less reliable in mountainous areas such as the basin and range terrain of northern Nevada than gently sloping land surfaces or over the ocean. The data sets and analysis methods used in this report are tailored to provide the most trust-worthy information available on the current and future climate of the Summit Lake, NV region.

Key findings for the Summit Lake, NV region are:

- For the period from 1990-2023, seasonal temperatures for June-July-August have increased by about 1 °F per decade. There were no notable temperature trends for the other seasons.
- There were no significant trends in seasonal precipitation accumulations between 1990 and 2023. The December-January-February season usually has the most precipitation and largest variations year to year.
- In the coming decades, it is likely that larger future temperature increases will occur during June-July-August as compared to the other seasons. Hot summer weather conditions may more frequently extend into September. The more likely scenario shows increases in June-July-August temperatures of ~ 0.5 °F/decade as compared to the low probability worst case scenario of ~ 1.6 °F/decade.
- December-January-February seasonal precipitation may increase slightly in the coming decades ($\sim$0.2 in/decade in the likely scenario and $\sim$0.5 in/decade in the low probability scenario). Large variability in year to year precipitation accumulation is likely to continue.

There is sparse information on historical conditions for the Summit Lake region. Predicting the future climate is very challenging and has large uncertainties. Definitive answers are not available.

Table of Contents

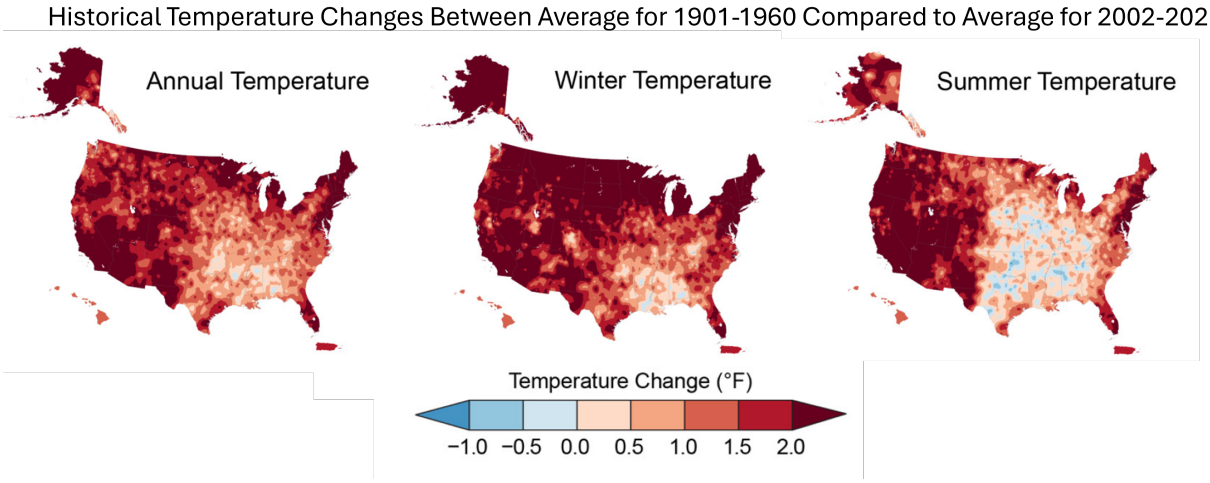

Figure 1: Observed historical changes in air temperatures in the United States since the first portion of the 20th century. Values are computed by subtracting regional average values from 2002-2021 from those from 1901-1960. Adapted from Figure 2.4 in 2023 US Climate Assessment (Crimmins et al., 2023).

1 Introduction

Projected climate changes in the news are commonly reported as global averages and as values over large continental regions (Intergovernmental Panel on Climate Change (IPCC), 2023; Crimmins et al., 2023). However, there is a lot of regional variation, so values for large areas are of limited use for local community climate adaptation planning.

Weather forecasts and climate predictions are generally less reliable in mountainous areas (such as the basin and range terrain of northern Nevada) than gently sloping land surfaces (such as the east coast of the US) or over the ocean (e.g. Berner et al., 2012; Maraun and Widmann, 2015; Kim et al., 2022). The difficulties arise in part from over-smoothing complex topography within the models. This over-smoothing reduces the heights of mountain peaks and ridges and removes smaller valleys, ridge gaps, and smaller lakes which are critical to air movement and humidity in the real world. Additionally, the chosen grid resolution of the model necessitates tradeoffs between more basic versus more detailed representations of earth system physical processes within models (e.g. Stevens et al., 2020).

The data sets and analysis methods used in this report are tailored to provide the most trustworthy information available on the current and future climate of the Summit Lake, NV region. As a consequence of the lower reliability of weather forecast model output in complex terrain, we base our analysis of historical weather over recent decades on weather station observations only. We cautiously utilize the lower reliability climate predictions in mountainous terrain.

For most of the statistics examined in this report, the calendar year was subdivided into three month seasons (December-January-February = DJF, March-April-May = MAM, June-July-August = JJA, and September-October-November = SON). Previous studies have shown that the magnitudes of regional climate variability often vary by season. For example, Crimmins et al. (2023) found for many regions in the US that between the first 60 years of the 1900s and the first two decades of the 2000s that winter season temperatures are warming faster than summer season temperatures and that some regions are cooling (Fig. 1).

1.1 Key Variables Defined

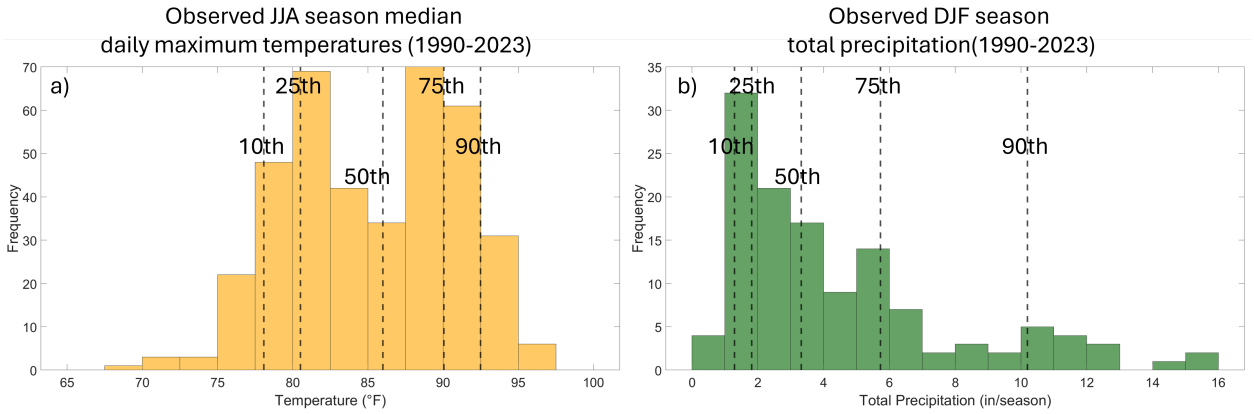

Figure 2: Example statistical distributions for Summit Lake region with percentile values annotated. (a) Observed June-July-August daily maximum temperatures (13 weather stations) have a bimodal distribution where the median value occurs less frequently than either the 25th or 75th percentiles. (b) Observed December-January-February seasonal precipitation (in/season) (5 weather stations) has a skewed distribution with the most frequently occurring values toward the low end as is typical for precipitation. Both of these distributions are non- Gaussian.

Distributions in statistics illustrate the frequency of specific data values within the entire set of data values. The *percentiles of the statistical distribution* are a way of distilling information on how the frequency varies by indicating *relative standing*. The *10th, 25th, 50th, 75th, and 90th percentiles* are commonly used in statistical analysis. For example, the 10th percentile represents that value below which 10% of the data fall. The the 25th percentile represents the value below which 25% of the data fall and so on. The 50th percentile corresponds to the *median*. Half the points are below this value and half are above it. Example distributions for seasonal temperatures and precipitation (Fig. 2) illustrate the locations of various percentile values. The *interquartile range* represents the difference between the 75th and 25th percentiles of the distribution. Overall, percentiles usually present a more representative picture of the characteristics of data values and their spread than the single minimum and single maximum in a data set. Minimum and maximum values could be outliers; unusual data points that are far removed from the rest of the data.

Median Absolute Deviation (MAD) indicates the typical y-axis distance (in the y axis variable's unit) on the time series plot between individual points and the median value. Higher MAD values indicate that the individual points tend to spread farther from the median (i.e. there is more variability) and lower values indicate a smaller spread. This statistic is better suited to analysis of temperature and precipitation data than standard deviation and mean absolute deviation since it can better handle outliers and non-Gaussian distributions.

To quantify *seasonal trends* in median daily minimum and maximum temperatures and total precipitation, we use two different trend estimates: simple linear regression and the Theil-Sen slope estimate. The Theil-Sen method for estimating a trend chooses the median slope from the slopes of all pairs of points, making this method of estimating trends more reliable in the presence of extreme observations. A permutation test is used to determine if the trends detected by simple linear regression and the Theil-Sen estimates are likely to be genuine or could be observed by chance alone. We first calculate the trend found in the observed data. Then we assume that there is no real trend, and repeatedly shuffle the order of data at random thousands of times. For each new random shuffle, we calculate the new trend, giving a distribution of trends created purely

by chance. If the actual trend has less than a 5% chance to be generated at random, then it is determined to not likely be observed by random chance, indicating the likely presence of a real, significant trend.

1.2 Annual cycle and seasonal cycle of temperatures

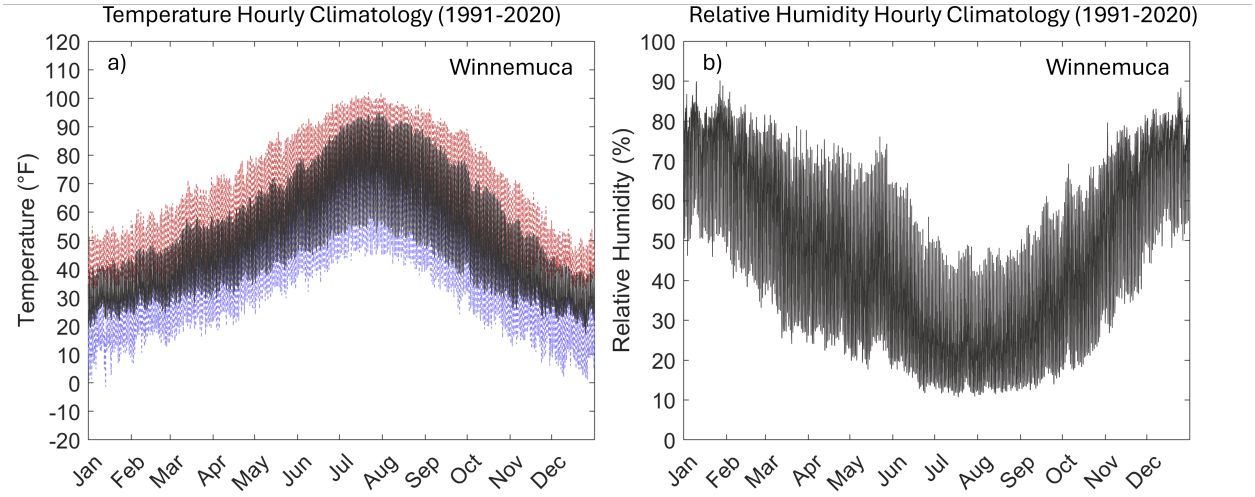

Figure 3: Annual variation of typical ranges of a) hourly temperatures and b) relative humidities at the Winnemuca, Nevada airport for each of 8760 hours in the year (excluding leap days) over the period 1991-2020. Black lines show mean temperatures each hour. Associated with the diurnal cycle, hourly values oscillate during each 24 hours, rising during the day and falling at night. Top edge of the band of black lines represents average high temperature and bottom edge of black lines represents average low temperature for a given date. For a) there is a 1 out of 10 chance that values in a given day and hour will be higher than the upper edge of the band defined by the red lines, and a 1 out of 10 chance that in a given day and hour the actual value will be lower than the bottom edge of the band defined by the blue lines.

Northern Nevada has a high desert climate. The 30-year (1991-2020) hourly climatology for Winnemuca, NV (Fig. 3) illustrates the seasonal cycle in hourly temperature and relative humidity for a typical year and their variations. Winnemuca (KWMC) is the closest airport to Summit Lake with a long-running weather station archiving hourly data. The highest temperatures occur in late July and early August and the lowest temperatures occur in late December and early January. Temperatures decrease at a faster rate between September and December as compared to the more gradual increases in temperatures between January to June. Hourly temperatures on a given day typically vary by 20 °F or more with the largest daily temperature ranges (about 40 °F) occurring during the summer (vertical spread of black lines in Fig. 3a).

Relative humidity varies with temperature and the moisture content of the air. If the moisture content stays the same, relative humidity decreases with increasing temperature. The annual cycle of relative humidity has the lowest values in the summer and highest values in the winter (Fig. 3b). Lower relative humidity reduces soil moisture, tends to dry out vegetation, and increases the potential for wildfires.

Since climate changes are not uniform throughout the year, dividing the year into seasons helps to isolate decadal trends. Figure 4 shows the ranges and frequencies of daily minimum and daily maximum temperatures by season for 1990-2023. There are two distinct modes in the combined season maximum temperature distribution. One centered near 40 °F and one centered near 80 °F. Over the entire year, daily maximum temperatures have a wide range ∼20 °F to ∼105 °F.

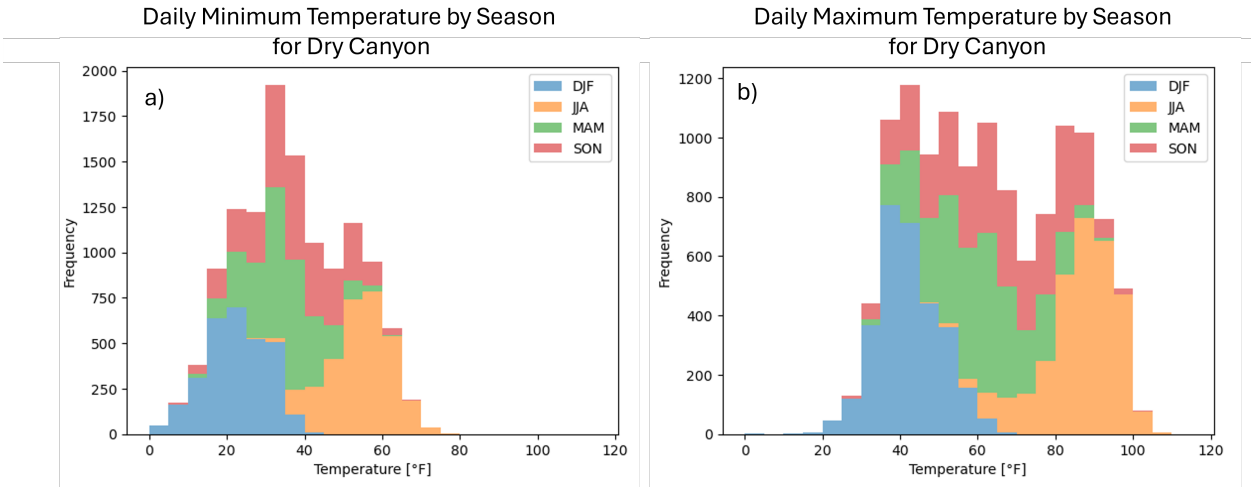

Figure 4: Stacked histograms of the seasonal distributions of a) daily minimum and b) daily maximum temperatures at Dry Canyon weather station (closest long-running weather station to Summit Lake). Each season is shown in a different color (see key). For each 5 °F temperature interval, frequencies within each season are added yielding the stacked bars. The period of analysis is from 1 Jan 1990 to 1 Jan 2024 (12,419 days).

Minimum daily temperatures for a given season have a smaller range of values than maximum daily temperatures. The most commonly occurring daily minimum temperatures in the "shoulder seasons" of September-October-November and March-April-May are between 30 °F and 40 °F (Fig. 4a).

2 Analysis of Historical Observations

2.1 Weather Station Data

The data used for the analysis of historical observations is from the Global Historical Climatology Network daily (GHCNd) database (Menne et al., 2012) hosted by the National Center for Environmental Information (NCEI). GHCNd is an integrated database of daily climate summaries from land surface stations across the globe. GHCNd is made up of daily climate records from numerous sources that have been integrated and subjected to quality assurance reviews (Durre et al., 2008, 2010). Primary GHCNd variables include daily maximum and minimum temperature values and daily total liquid-equivalent precipitation accumulation. GHCNd data are not corrected for instrument or location related biases but they are reviewed for nonsensical values and spatial consistency.

There were 36 weather stations that had some data for period 1900-2025. In the trend analysis, we only used the subset of 13 weather stations that had nearly continuous records from 1990 to 2023 (Table 1, Fig. 5). For a given 3 month season for a given year, the weather station had to have >= 90% of days recorded to be included in the analysis.

Reanalysis products such as ECMWF's reanalysis version 5 (ERA5) are often used to look at historical weather. Reanalysis combines weather forecasts rerun for past periods with observations to yield gridded maps. In locations where the weather forecast model has larger errors such as mountainous areas, the reanalysis' observation assimilation weights the available observations less so biases remain large (Parker, 2016). Upon close inspection of these products for the northern

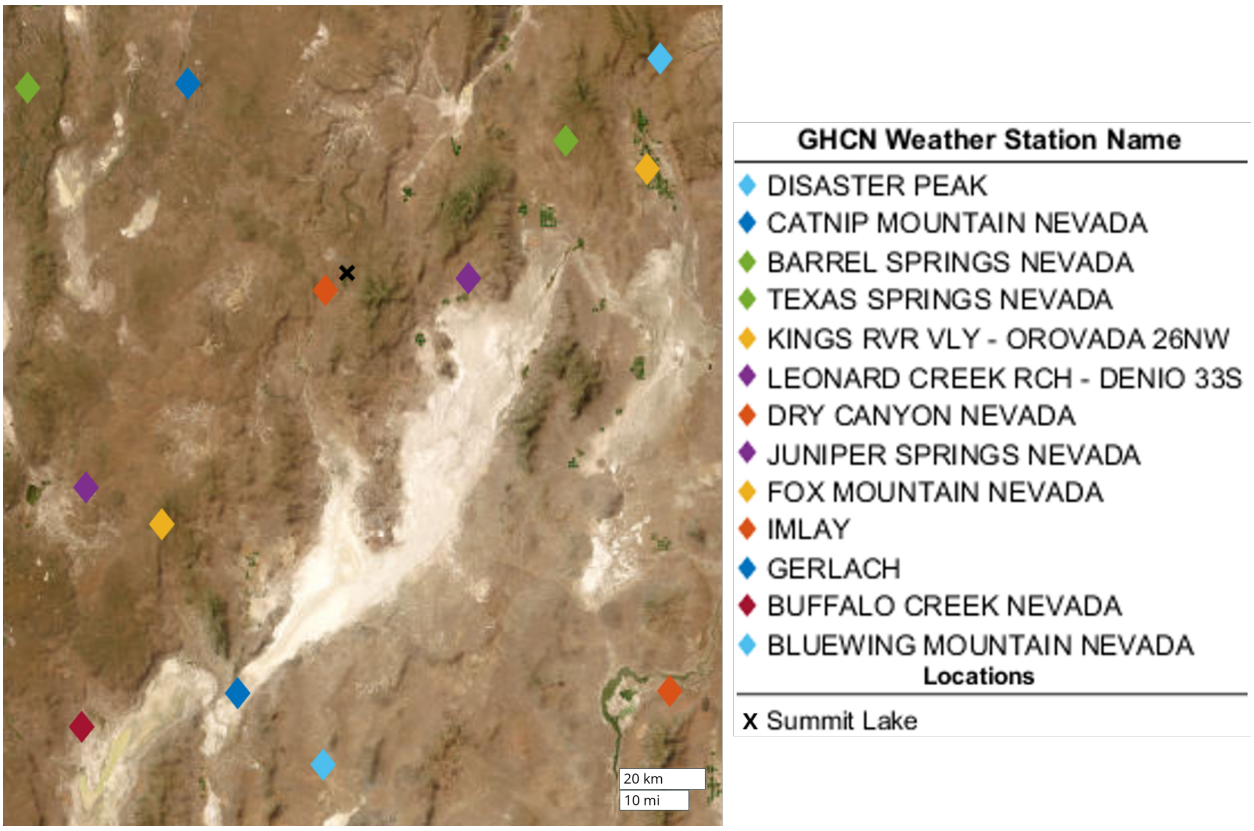

Figure 5: Map of Summit Lake region showing the 13 weather stations within the $\pm 1^\circ$ latitude and $\pm 1^\circ$ longitude region used for the historical analysis. x shows position of Summit Lake. Map is cut off at $\sim 42^\circ$ N since there are no weather stations within 1° of Summit Lake north of that latitude. Stations are listed from northern most (Disaster Peak) to southern most (Bluewing Mountain). See Table 1 for detailed information on each station. The 5 weather stations with precipitation data used in the analysis are Disaster Peak, Kings River Valley, Leonard Creek Ranch, Imlay, and Gerlach.

Nevada region, we concluded that they are not sufficiently reliable enough to use in our analysis. In particular, we found that the spatial patterns of precipitation for northern Nevada were implausible, which brought into question the quality of the temperatures as well. Hence, we chose not to include ERA5 reanalysis products in this analysis.

2.2 Recent Decadal Trends and Variability

Information on the historical observations of temperature and precipitation are presented with time series graphs showing the median weather station values for each weather station and each year (Figs. 6, 7, and 8). Statistics derived from these time series on the variability and trend numerical values are shown in Tables 2 and 3.

Table 2 shows the percentiles and variability of historical daily minimum and daily maximum temperatures and seasonal liquid-water equivalent precipitation as well as mean values. Comparing among distribution statistics allows us to quantify key differences among the seasons. December-January-February has the largest range between the 90th and 10th percentiles in seasonal precipitation (10.2 in to 1.1 in) and June-July-August (2.7 in to 0.2 in) the smallest. Regionally, the "shoulder" season of March-April-May has the largest difference between the 90th and 10th percentiles for daily maximum temperature (18 °F). In comparison the largest relative

Station Name	Latitude	Longitude	Elevation (ft)
Disaster Peak, NV	41.9700°N	118.1900°W	6500
Catnip Mountain, NV	41.9200°N	119.4950°W	5740
Barrel Springs, NV	41.9111°N	119.9389°W	5835
Texas Springs, NV	41.8017°N	118.4508°W	5760
Kings River Valley - Orovada, NV	41.7436°N	118.2258°W	4240
Leonard Creek Ranch - Denio, NV	41.5167°N	118.7192°W	4239
Dry Canyon, NV	41.4917°N	119.1167°W	4900
Juniper Springs, NV	41.0819°N	119.7772°W	5348
Fox Mountain, NV	41.0061°N	119.5681°W	6890
Imlay, NV	40.6564°N	118.1631°W	4260
Gerlach, NV	40.6517°N	119.3578°W	3954
Buffalo Creek, NV	40.5819°N	119.7900°W	2794
Bluewing Mountain, NV	40.5017°N	119.1217°W	4570

Table 1: Locations and elevations for the 13 weather stations in the Summit Lake vicinity (Figure 5) with nearly complete temperature records from 1990-2023 (less than 10% missing data). Stations are listed from north to south. Dry Canyon is the station with a long data record closest to Summit Lake. The 5 weather stations with nearly complete precipitation data used in the analysis are Disaster Peak, Kings River Valley, Leonard Creek Ranch, Imlay, and Gerlach.

differences for daily minimum temperatures are roughly half that value.

The Theil-Sen and linear regression trend calculations yield very similar results for the historical record (Table 3). There are some differences between the two fit calculations for precipitation but it does not matter since there are no significant trends in precipitation overall.

Historical Variability (1990-2023)

Variable	Season	Mean	Median	Median Absolute Deviation	Interquartile Range	90th Percentile	10th Percentile
Accum Precip	DJF	4.50	3.32	1.74	3.91	10.19	1.30
Accum Precip	MAM	3.47	2.87	1.44	2.96	6.74	0.93
Accum Precip	JJA	1.23	1.09	0.65	1.40	2.67	0.16
Accum Precip	SON	2.29	1.79	0.83	1.83	4.41	0.65
Temp Max	DJF	41.1	41.0	3.3	6.8	46.9	35.7
Temp Max	MAM	57.8	57.9	5.9	11.5	66.9	48.9
Temp Max	JJA	85.4	86.0	5.0	9.5	92.5	78.1
Temp Max	SON	63.5	64.0	4.9	9.0	71.1	55.9
Temp Min	DJF	23.5	24.1	2.2	5.0	28.0	18.7
Temp Min	MAM	34.2	34.0	2.0	4.1	39.0	30.4
Temp Min	JJA	54.5	55.0	2.5	5.0	59.0	50.0
Temp Min	SON	37.8	37.9	2.5	4.9	42.6	33.1

Table 2: Table summarizing recent historical climate variability (1990-2023) for median seasonal minimum and maximum temperatures (°F) and accumulated precipitation (inches over the 3 month season) for Summit Lake, NV, region. For seasonal accumulated precipitation, only 5 stations were included, for seasonal median temperatures, all 13 stations were used (see Figure 5).

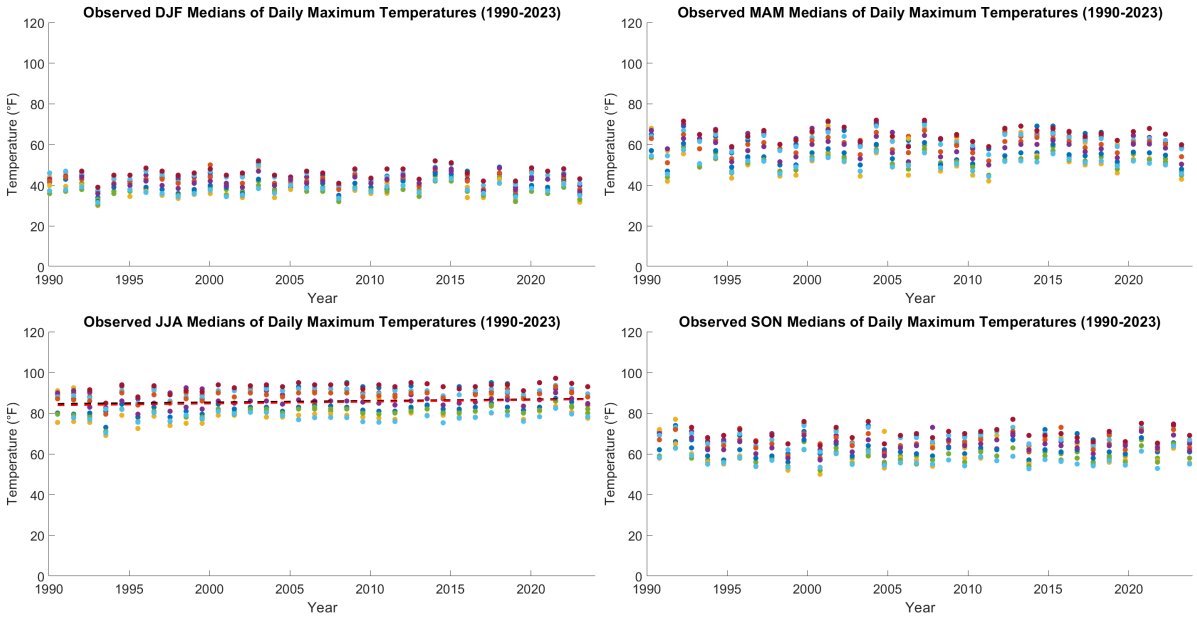

Figure 6: 1990-2023 time series for seasonal temperature maximum for the 13 weather stations near Summit Lake. Each colored dot in a given year corresponds to a weather station in Figure 5 (Table 1). Only the trend for June-July-August ($\sim$0.8°F/decade) is significant. Dashed lines indicate linear fit (orange) and Theil-Sen fit (black). These fitted lines are nearly identical (Table 3).

Historical Trends (1990-2023)

Variable	Season	Theil-Sen Trend (per decade)	Theil-Sen Significance Test p-value	Linear Trend (per decade)	Linear Significance Test p-value
Accum Precip	DJF	0.23	0.4722	0.20	0.6232
Accum Precip	MAM	-0.02	0.9556	-0.10	0.7546
Accum Precip	JJA	-0.07	0.6144	-0.08	0.5324
Accum Precip	SON	0.15	0.3232	0.11	0.5240
Temp Max	DJF	0.00	1.0000	0.22	0.6734
Temp Max	MAM	-0.23	0.6750	-0.26	0.6990
Temp Max	JJA	**0.75**	0.0260*	**0.89**	0.0168*
Temp Max	SON	0.00	1.0000	0.00	0.9788
Temp Min	DJF	0.00	1.0000	0.33	0.4606
Temp Min	MAM	-0.19	0.3976	-0.30	0.3734
Temp Min	JJA	**1.23**	0.0002*	**1.27**	0.0002*
Temp Min	SON	0.47	0.1880	0.52	0.1868

Table 3: Table summarizing recent historical trends (1990-2023) for median seasonal minimum and maximum temperatures (°F/decade) and accumulated precipitation (inches/decade) for Summit Lake, NV, region. Significant trends as detected by permutation testing indicated in bold. Significant p-values indicated with an (*). For seasonal accumulated precipitation, only 5 stations were included, for seasonal median temperatures, all 13 stations were used (see Figure 5).

2.3 Findings for 1990-2023

Based on the recent historical record of weather station observations in the Summit Lake region:

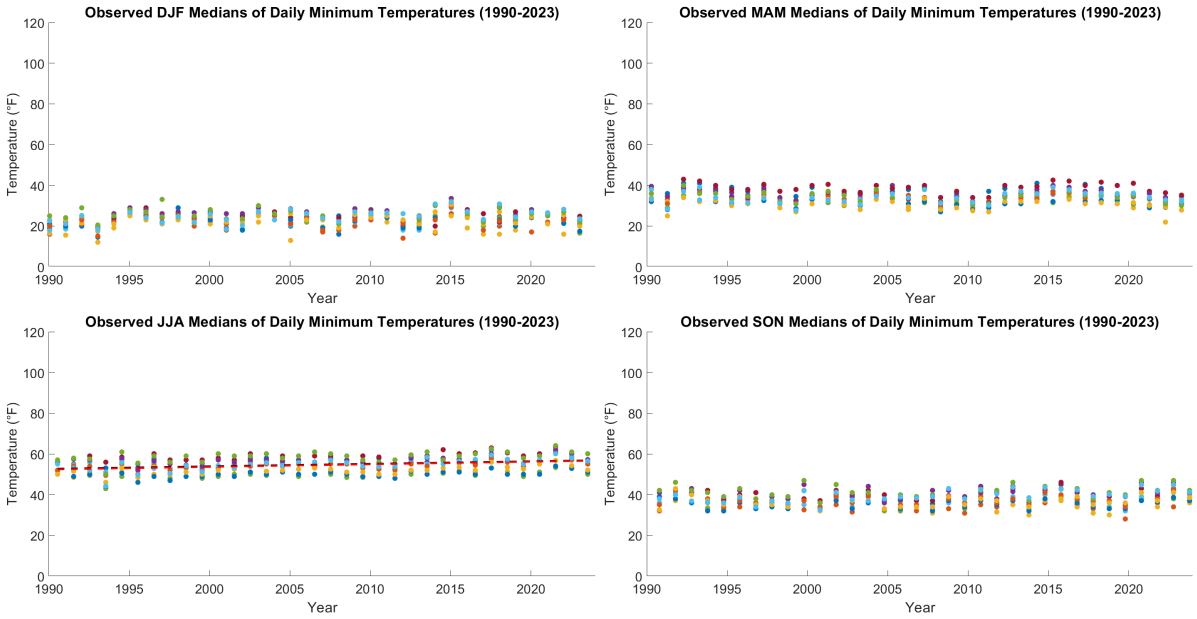

Figure 7: 1990-2023 time series for seasonal temperature minimum for the 13 weather stations near Summit Lake. Each colored dot in a given year corresponds to a weather station in Figure 5 (Table 1). Only the trend for June-July-August ($\sim$1.3°F/decade) is significant. Dashed lines indicate linear fit (orange) and Theil-Sen fit (black). These fitted lines are nearly identical (Table 3).

- The June-July-August season had clear trends for increasing temperatures. A larger trend of $\sim$1.3° F/decade for temperature minimum and $\sim$0.8° F/decade for temperature maximum. There were no significant temperature trends for the other seasons.
- No notable trends in seasonal liquid-equivalent precipitation accumulation. All seasons had large year-to-year variability of precipitation.
- December-January-February usually has the highest seasonal precipitation but amounts can vary from over 10 inches in a wet year to less than 1.3 inches a dry year.

The limitation of only 5 weather stations with complete enough precipitation records to do the analysis for 1990-2023 yields less confidence in the precipitation results as compared to the results for temperatures which are based on 13 weather stations.

3 Analysis of Climate Projections

Climate models are designed to yield information on long-term average conditions as well as the likelihood of extreme events over time scales of decades or more. They aim produce the right types and frequencies of weather events but not specific forecasts of day to day weather. Hence while climate models output maps for individual days, the map for a specific day, say 15 Jan 2035, that shows a storm off the coast of California, is not intended to be interpreted to represent the occurrence of a storm in that location on that day. This is contrast to weather models which are designed to provide day to day and hour to hour forecasts for specific days and locations.

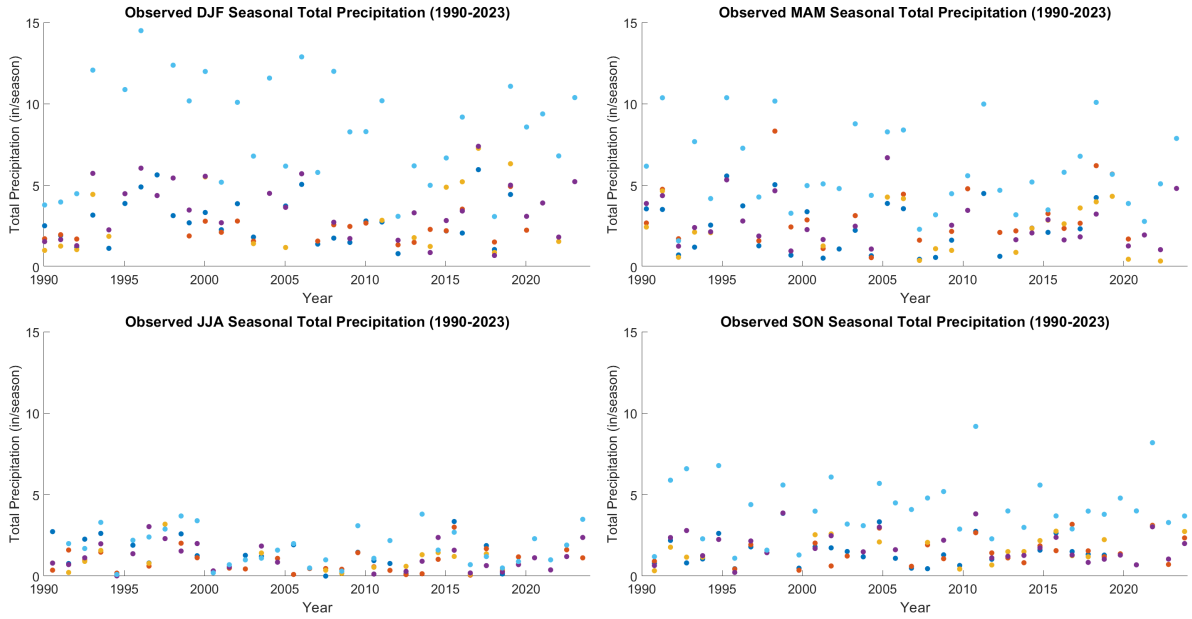

Figure 8: 1990-2023 time series for seasonal precipitation accumulation (inches over the 3 month season) for the 5 weather stations with long precipitation records near Summit Lake. Each colored dot in a given year corresponds to a different station. Some dots have nearly the same value and are hard to distinguish. There are no significant trends in these data. The station with the highest seasonal accumulations in most years for December-January-February, March-April-May, and September-October-November is Disaster Peak, NV.

3.1 Explanation of Input Emission Scenarios

Climate projections vary based on their inputs and how they estimate key physical processes and feed backs in atmosphere-land-ocean-ice system (e.g. Frassoni et al., 2023). Climate scientists have found that their temperature projections are most sensitive to the input values of estimated global CO_2 concentrations in the atmosphere (Zhang et al., 2023). The estimated total concentration in a given year represents the CO_2 concentration from the previous year plus the net CO_2 emitted that year minus CO_2 removed. CO_2 can be removed from the atmosphere by green plants (including forests and algae), soils, carbon mineralization, and technologies such as direct air capture. Emission scenarios are based on modeled predictions of future global economics, policies, and anticipated progress in carbon dioxide reduction and removal techniques.

Emissions scenarios are named based on the representative concentration pathway (RCP) they were crafted to explore (Fig. 9). Each RCP is defined by its radiative forcing value in the year 2100 (measured in watts per square meter) which represents the additional energy trapped in the Earth system compared to preindustrial levels due to greenhouse gases and other factors. The current set of RCPs were developed for the IPCC's Fifth Assessment Report (Intergovernmental Panel on Climate Change (IPCC), 2014) using computer models that combine economic, energy, land-use, and climate systems. They are plausible "storylines" based on specific assumptions, not fixed forecasts. Two emission scenarios have been most studied and these are the ones we use in this report.

RCP 4.5 – A more likely CO_2 emission scenario with radiative forcing of $\sim$4.5 W/m^2 ($\sim$650 ppm CO_2 concentration equivalent) in 2100. The scenario's design goal was to represent CO_2 stabilization without overshoot wherein greenhouse gas concentrations level off by mid-to-late century due to a "moderate" climate policy which features significant emissions reductions starting around

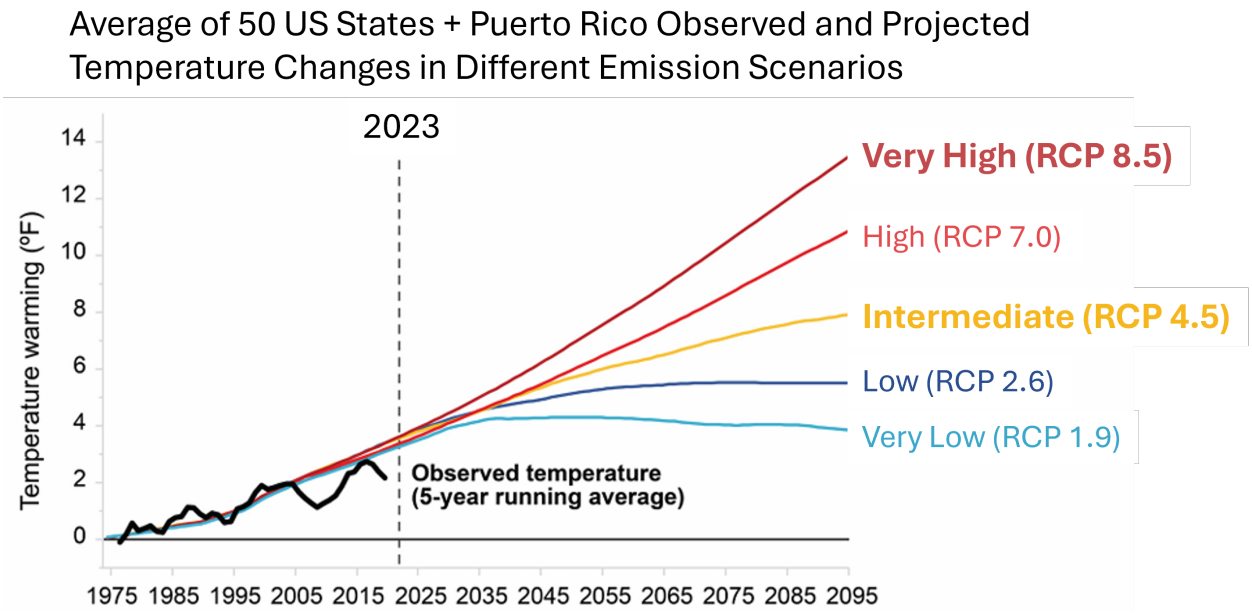

Figure 9: Comparison of projected average annual temperatures relative to the value in 1976 for different emission scenarios (RCPs) combining data from the 50 US states and Puerto Rico. Black line shows observed temperatures and other colors indicate different emission scenarios. This report focuses on the RCP 4.5 (yellow line) and RCP 8.5 (dark red line) emission scenarios. Adapted from Figure 1.13 in the 2023 US Climate Assessment (Crimmins et al., 2023).

2040, reduced fossil fuel usage over time and more climate-focused agricultural and land use practices. This scenario yields a US average temperature change between 2023 and 2095 of ∼5°F.

RCP 8.5 – A low probability, worse-case CO_2 emission scenario with radiative forcing of ∼8.5 W/m^2 (∼1370 ppm CO_2 concentration equivalent) in 2100. The design goal of this RCP was to represent a scenario with no actions toward curbing greenhouse gas emissions and a continuing acceleration in their emissions by increasing numbers of coal power plants. This scenario yields a US average temperature change between 2023 and 2095 of ∼10°F. While the very high CO_2 emissions in this scenario are considered unrealistic by most climate scientists, the RCP 8.5 scenario is used as a workaround to glean information about potential earth system feedbacks that are known to be poorly represented in climate models.

According to US National Oceanographic and Atmospheric Administration websites, as of October 2025, current CO_2 levels in the atmosphere are ∼425 ppm. In 1990, values were close to ∼355 ppm. CO_2 increased by 3.75 ppm in 2023 which was the highest one year increase on record. If that high rate continues through 2100 it would yield a CO_2 concentration of ∼714 ppm in 2100. Many countries, particularly China, are in the process of increasing their use of renewable energy sources to generate electricity which will contribute to reducing the rate of global CO_2 emissions per year compared to the 2023 rate. Based on current policies and predicted technological progress, net-zero emissions (greenhouse gas emissions = removals in a given year) are anticipated to be achieved globally sometime between 2050 and 2100.

3.2 Cal-Adapt LOCA Climate Models

The climate model data used in this study were obtained from Cal-Adapt (cal-adapt.org), a organization run by the California Energy Commission to make climate information more accessible

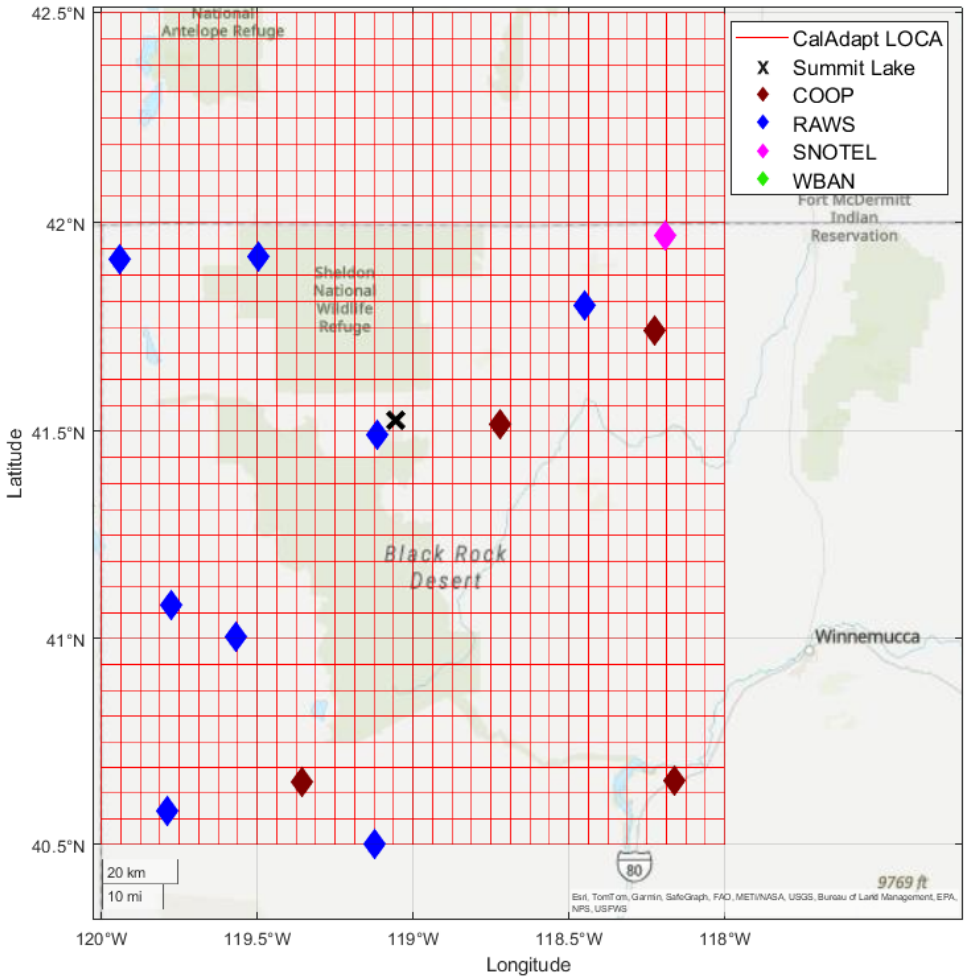

Figure 10: Map of Summit Lake region showing weather stations (8 RAWS, 4 COOP, and 1 SNOTEL) within ±1 deg latitude x ±1 deg longitude of Summit Lake and the corresponding ∼6 km x ∼6 km grid boxes for LOCA downscaled climate projections (red).

and actionable for a broad audience. The Cal-Adapt website provides climate model data derived from the Climate Model Intercomparison Project 5 (CMIP5) which was commissioned as part of the reports generated by the Intergovernmental Panel on Climate Change (IPCC). The CMIP5 climate models were downscaled using the LOCA (Localized Constructed Analogs) technique. Downscaling uses statistical methods to change the grid spatial resolution from ∼200 km x ∼200 km of CMIP5 to ∼6 km x ∼6 km for LOCA (Pierce et al., 2014). LOCA ∼6 km x ∼6 km grid boxes and weather station in the vicinity of Summit Lake are shown in Figure 10.

Cal-Adapt did further calculations for their focus area of California and Nevada with the statistically downscaled climate data. The regionally subset data was also used to force a variable infiltration model (LOCA-VIC) which produces such quantities as runoff, snow cover, surface long- and short-wave radiation, and soil moisture.

Starting in the year 2007 through to 2100 the climate models used in this analysis are run

forward in "prediction" mode. They do not use information from observations from 2007 to the present day. We first examined climate projections from all 32 models available from Cal-Adapt. For a given emissions scenario, there were usually only minor differences among the predictions which is not surprising since many of the climate modeling centers use similar or identical programming code to represent key physical processes. Pierce et al. (2018) identified a subset of four climate models whose projected future climate can be described as producing: 1) a “warm/dry” simulation; 2) an “average” simulation; 3) a “cooler/wetter” simulation; 4) the model simulation that is most unlike the first 3 (for the best coverage of different possibilities). All simulations show future warming. The “cooler” simulation show less warming than other models. HadGEM2-ES is the “warm/dry” model, CanESM2 is the “average” model, CNRM-CM5 is the “cool/wet” model, and MIROC5 is the model that has the pattern that is most unlike the other three models and was chosen to give better coverage of the full spread of global climate model results. However, when we did our statistical analysis for the northern Nevada region, we found only minor differences among the projections from these four models. For presentation purposes, we focus on just the CanESM2 "average" model since the quantitative statistical values we compute are very similar to the other three highlighted models in Pierce et al. (2018).

3.3 Findings for 2030-2099

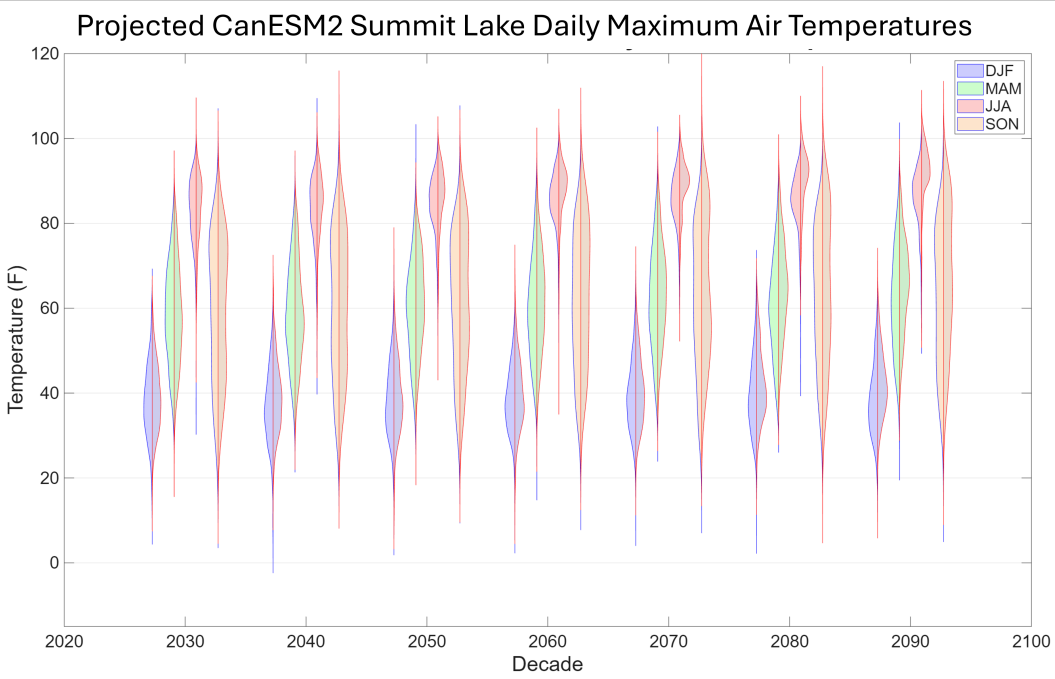

Figure 11: Summit Lake future (2030-2099) seasonal maximum temperature predictions by decade from "average" model CanESM2. Data are from the LOCA grid box closest to Summit Lake and are subset by decade and by season. For each decade, the distributions of future values are shown as violin plots with the left side indicating the more likely climate scenario (RCP 4.5) and the right side indicating the low probability very hot climate scenario (RCP 8.5).

Since carbon dioxide concentrations accumulate over time and increase at a faster rate for RCP 8.5 as compared to RCP 4.5, the prediction differences between the two emission scenarios are small for 2030s and diverge more for 2090s. To keep comparisons between the historical observa-

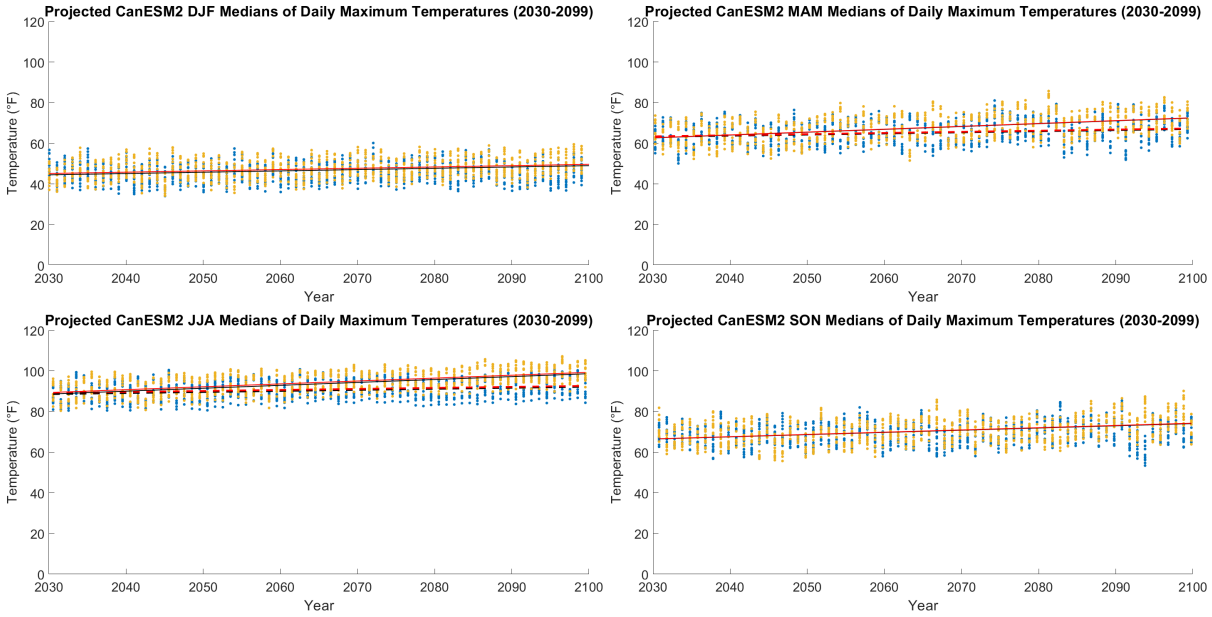

Figure 12: Summit Lake future (2030-2099) seasonal maximum temperature time series with trends from "average" model CanESM2. The more likely climate scenario (RCP 4.5) is indicated by blue dots. The low probability very hot climate scenario (RCP 8.5) is indicated by yellow dots. RCP 4.5 has a significant trends for March-April-May and June-July-August (dashed lines). RCP 8.5 has significant trends for all seasons (solid lines). See Table 4 for trend numerical values.

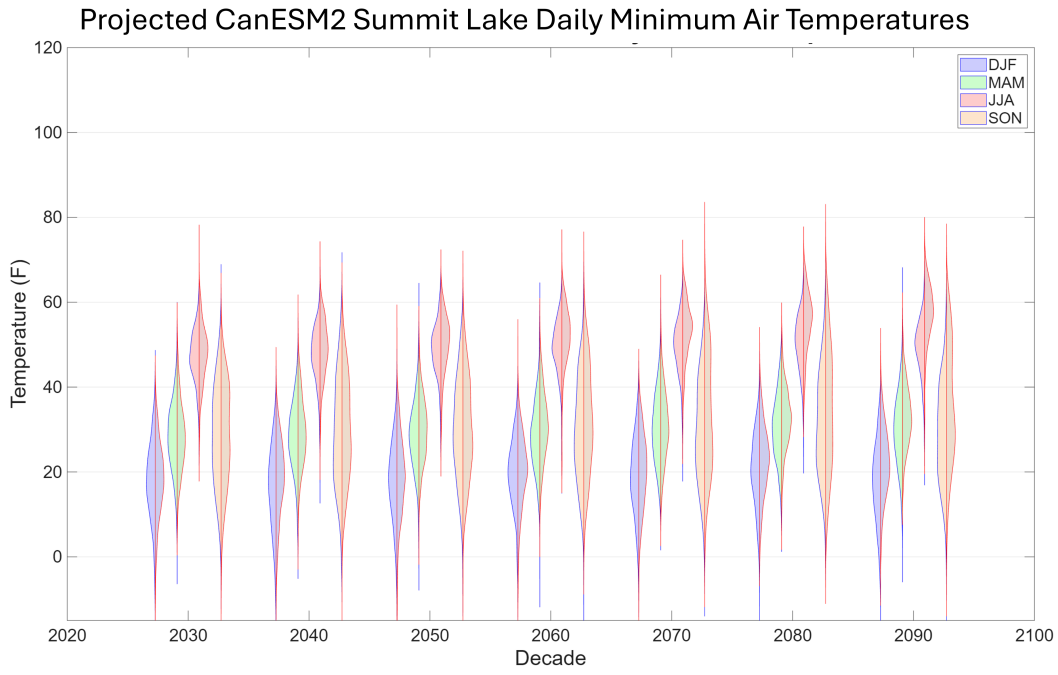

Figure 13: Summit Lake future (2030-2099) seasonal minimum temperature predictions by decade from the "average" model CanESM2. Data are from the LOCA grid box closest to Summit Lake and are subset by decade and by season. For each decade, the distributions of future values are shown as violin plots with the left side indicating the more likely climate scenario (RCP 4.5) and the right side indicating the low probability very hot climate scenario (RCP 8.5).

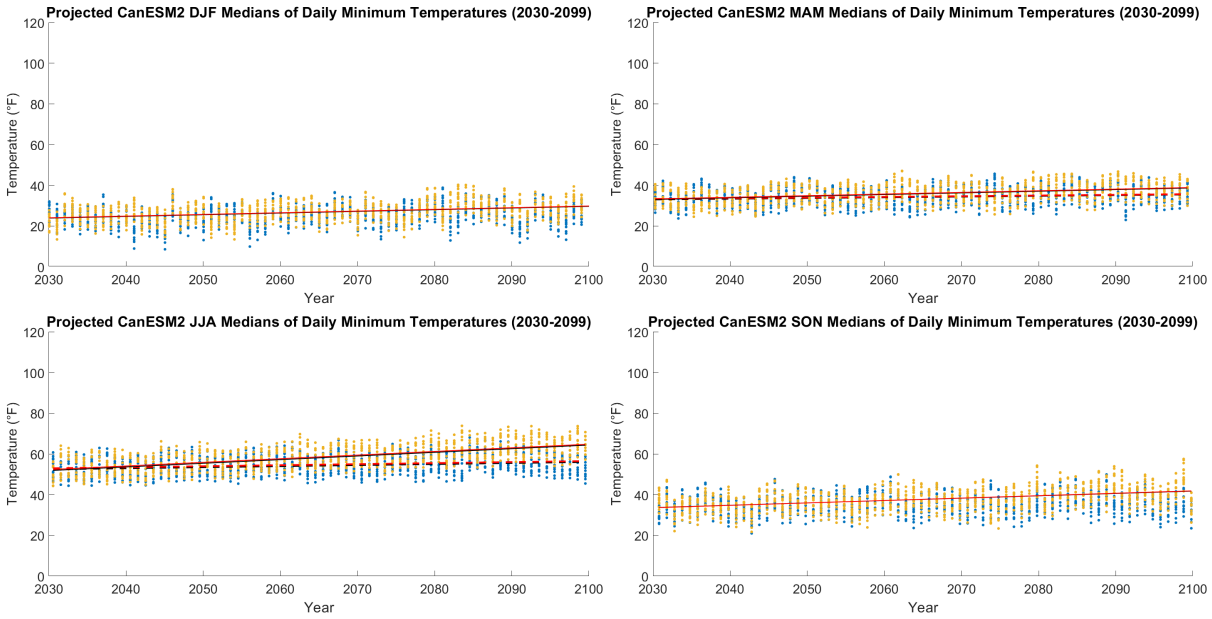

Figure 14: Summit Lake future (2030-2099) seasonal minimum temperature time series with trends from "average" model CanESM2. The more likely climate scenario (RCP 4.5) is indicated by blue dots. The low probability very hot climate scenario (RCP 8.5) is indicated by yellow dots and solid lines. RCP 4.5 has a significant trend only for June-July-August (dashed line). RCP 8.5 has significant trends for all seasons (solid lines). See Table 4 for trend numerical values.

tions and climate predictions consistent, we use the climate model grid locations corresponding to the weather stations (Fig. 10).

We present the climate projections for our three variables (seasonal minium temperatures, seasonal maximum temperature, and seasonal liquid-equivalent precipitation accumulation) using two types of graphs. Sets of violin plots (Figs. 11 and 13) illustrate the *ranges* of temperature projections for each 10 year period from 2030 to 2099. For each decade (2030-2039, 2040-2049 etc.), distributions for each season are displayed vertically in pairs with the left side representing the more likely RCP 4.5 scenario and the right side showing the less likely RCP 8.5 scenario.

Time series plots (Figs. 12, 14, and 15) show the sequence of median values for each season in each year with different dots for a given year representing different weather station locations. Blue dots indicate the RCP 4.5 and and yellow dots indicate RCP 8.5 scenarios. These data are used to estimate the rate of increases in terms of trend lines fit for the entire 2030-2099 period. Both the linear regression and Thein-Sen trend lines are shown but the numerical values are so close to one another (Table 4) that they are difficult to distinguish in the plots.

3.3.1 Future Temperatures

Comparing among decades one can see a gradual increase in temperatures as the distributions for each season shift upward on the plots to higher values (Figs. 11 and 13). In the maximum temperature data, the high end of the distributions for September-October-November overlap a bit more with June-July-August at the end of the century as compared to 2030. This suggests that hot summer weather conditions may more frequently extend into September in the future. The differences between RCP 4.5 and 8.5 are small and barely noticeable for 2030 in both the violin and time series plots (Figs. 12 and 13). Starting in 2060, the offset between the two scenarios for

June-July-August is clearly distinct. The differences between the RCP scenarios is more subtle for the other seasons until 2090. Consistent with what the weather observation data shows for recent decades, in the future it is likely that the fastest warming will be in June-July-August as compared to the other seasons (Table 4).

Future CanESM2 Trends (2030-2099)

Variable	Season	RCP	Theil-Sen Slope (per decade)	Theil-Sen Significance Test p-value	Linear Slope (per decade)	Linear Significance Test p-value
Accum Precip	DJF	RCP 4.5	**0.19**	0.0380*	**0.23**	0.0408*
Accum Precip	DJF	RCP 8.5	**0.48**	0.0006*	**0.59**	0.0004*
Accum Precip	MAM	RCP 4.5	-0.03	0.6278	0.04	0.6852
Accum Precip	MAM	RCP 8.5	-0.01	0.8740	-0.03	0.7262
Accum Precip	JJA	RCP 4.5	0.08	0.2354	0.11	0.1258
Accum Precip	JJA	RCP 8.5	**0.25**	0.0016*	**0.23**	0.0028*
Accum Precip	SON	RCP 4.5	-0.08	0.2346	-0.09	0.2172
Accum Precip	SON	RCP 8.5	0.09	0.2038	0.08	0.4032
Temp Max	DJF	RCP 4.5	0.17	0.1706	0.16	0.1998
Temp Max	DJF	RCP 8.5	**0.65**	0.0002*	**0.64**	0.0002*
Temp Max	MAM	RCP 4.5	**0.55**	0.0034*	**0.56**	0.0040*
Temp Max	MAM	RCP 8.5	**1.40**	0.0002*	**1.41**	0.0002*
Temp Max	JJA	RCP 4.5	**0.52**	0.0002*	**0.50**	0.0002*
Temp Max	JJA	RCP 8.5	**1.43**	0.0002*	**1.42**	0.0002*
Temp Max	SON	RCP 4.5	0.36	0.0740	0.36	0.0802
Temp Max	SON	RCP 8.5	**1.09**	0.0002*	**1.10**	0.0002*
Temp Min	DJF	RCP 4.5	0.22	0.2846	0.19	0.3592
Temp Min	DJF	RCP 8.5	**0.83**	0.0002*	**0.83**	0.0002*
Temp Min	MAM	RCP 4.5	**0.35**	0.0052*	**0.34**	0.0062*
Temp Min	MAM	RCP 8.5	**0.81**	0.0002*	**0.80**	0.0002*
Temp Min	JJA	RCP 4.5	**0.52**	0.0002*	**0.51**	0.0002*
Temp Min	JJA	RCP 8.5	**1.79**	0.0002*	**1.78**	0.0002*
Temp Min	SON	RCP 4.5	0.18	0.2034	0.19	0.2068
Temp Min	SON	RCP 8.5	**1.16**	0.0002*	**1.19**	0.0002*

Table 4: Table summarizing CanESM2 "average model" projected trends for median seasonal minimum and maximum temperatures (°F/decade) and accumulated precipitation (in/decade) for Summit Lake, NV, region. Significant trends as detected by permutation testing indicated in bold. Significant p-values indicated with an (*). For seasonal accumulated precipitation, only 5 weather station locations were included, for seasonal median temperatures, 13 weather station locations were used.

3.3.2 Future Seasonal Precipitation

Similar to the large variability in precipitation accumulations for the historical period, there is likely to be continued large variability in seasonal precipitation accumulations year to year in the future (Fig. 15). Notable increasing trends are only present in December-January-February and June-July-August (Fig. 15). For RCP 4.5, a significant trend is present in December-January-February of $\sim$0.2 in/decade. For RCP 8.5, December-January-February has an increase of $\sim$0.54 in/decade and June-July-August has an increase of $\sim$0.24 in/decade (Table 5). The statistics and graphs for future precipitation suggest that under the more likely RCP 4.5 scenario that typical

December-January-February seasonal precipitation will increase slightly and that the likelihood of a given winter season with more than 5 inches of liquid-equivalent precipitation will increase.

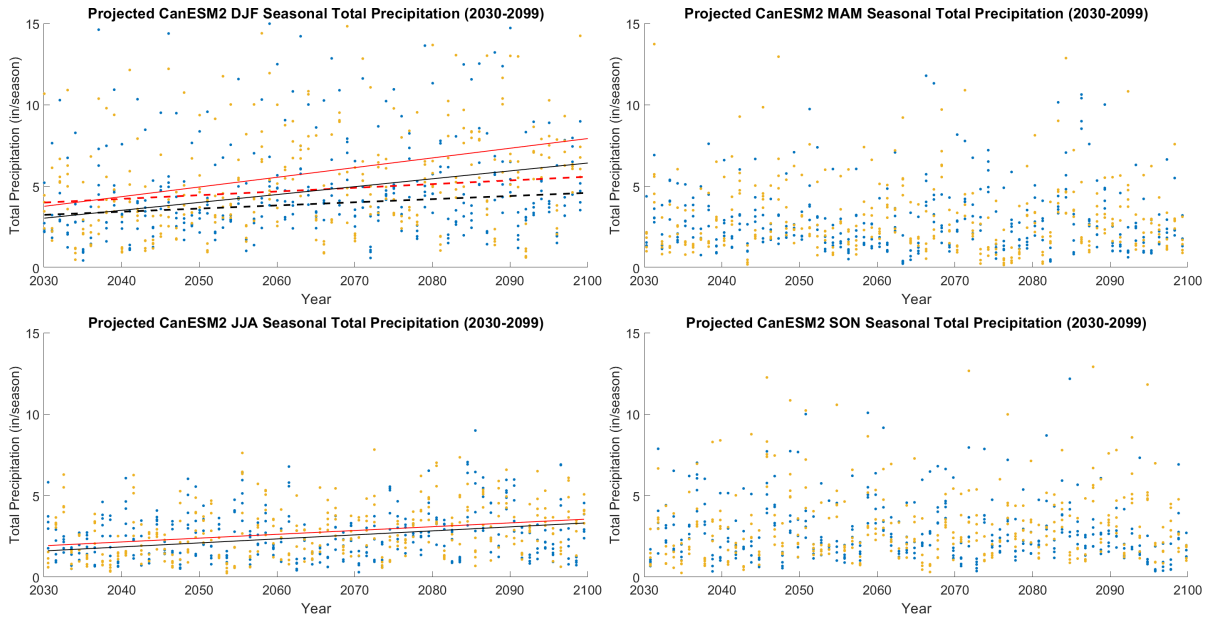

Figure 15: Summit Lake future (2030-2099) seasonal liquid-equivalent precipitation time series with trends from "average" model CanESM2. Data corresponding to the 5 locations with long-term precipitation records are shown for each RCP scenario in each year. The more likely climate scenario (RCP 4.5) is indicated by blue dots. The low probability very hot climate scenario (RCP 8.5) is indicated by yellow dots. RCP 4.5 has a significant trends for only December-January-February (dashed lines). RCP 8.5 has significant trends for December-January-February and June-July-August (solid lines). See Table 4 for trend numerical values.

Variable	Season	MAD (1990-2023)	RCP 4.5 MAD (2030-2065)	RCP 4.5 MAD (2066-2099)	RCP 8.5 MAD (2030-2065)	RCP 8.5 MAD (2066-2099)
Accum Precip	DJF	1.74	1.20	1.34	1.63	2.44
Accum Precip	MAM	1.44	0.82	1.20	1.06	1.06
Accum Precip	JJA	0.65	0.93	1.01	0.92	1.01
Accum Precip	SON	0.83	1.02	0.79	1.10	1.11

Table 5: Comparison of the precipitation variability for different time periods in terms of median absolute deviation (MAD) of accumulated seasonal precipitation. Values are for the observed historical period of 1990-2023 (Fig. 8), and the CanESM2 RCP 4.5 and RCP 8.5 model projections for the periods 2030-2065 and 2066-2099 (Fig. 15). RCP 4.5 variability for DJF and MAM may be underestimated since values are lower than for the recent historical period. Uses the 5 weather station locations from the historical period for the projected values.

4 Summary and Recommendations

As Yogi Berra stated, "It's tough to make predictions, especially about the future." Climate model outputs should be viewed less as definitive predictions than as illustrative scenarios that bracket

a range of more plausible to less plausible futures. Their strength lies in exploring the sensitivity of the earth system to changes in the concentrations of greenhouse gases, not in providing geographically specific forecasts. Climate modeling centers continue to refine their representations of earth system physics. Economists are working to improve their economic models that feed into emission scenarios. These changes tend to be incremental.

We looked at several options for historical and future climate data sets to base this report and selected those that in our judgment would provide the most trustworthy information available on the current and future climate of the Summit Lake region. Key findings from the historical observations and climate prediction data sets analyzed for this report are:

- For the period from 1990-2023, seasonal temperatures for June-July-August have increased by about 1 °F per decade. There were no notable temperature trends for the other seasons.
- There were no significant trends in seasonal precipitation accumulations between 1990 and 2023. The December-January-February season usually has the most precipitation and largest variations year to year.
- In the coming decades, it is likely that larger future temperature increases will occur during June-July-August as compared to the other seasons. Hot summer weather conditions may more frequently extend into September. The more likely scenario shows increases in June-July-August temperatures of ~ 0.5 °F/decade as compared to the low probability worst case scenario of ~ 1.6 °F/decade.
- December-January-February seasonal precipitation may increase slightly in the coming decades ($\sim$0.2 in/decade in the likely scenario and $\sim$0.5 in/decade in the low probability scenario). Large variability in year to year precipitation accumulation is likely to continue.

Heat stress starts to be felt by people, animals, and plants when temperatures exceed 86 °F (Sugg et al., 2016; Akbar et al., 2021). Average summer temperatures for Summit Lake region in recent decades are close to this threshold (Table 2). The number of hours above the heat stress threshold is likely to increase in future decades. Infrastructure designs that reduce temperatures in public spaces and within buildings would help to decrease health risks from heat stress.

In the near term, it is recommended that additional resources at the state and local level be found and allocated to increase the number of weather stations in northern Nevada. Particularly useful will be weather stations that include wind-shielded precipitation gauges. An enhanced regional weather network will permit better monitoring of climate changes as they occur in the coming decades.

References Cited

Akbar, S., and Coauthors, 2021: Heat stress and its management in dairy cattle: Current scenario in south asia. *Pakistan J Agric Res*, **34**, 407–413, doi:10.17582/journal.pjar/2021/34.2.407.413.

Berner, J., T. Jung, and T. N. Palmer, 2012: Systematic Model Error: The Impact of Increased Horizontal Resolution versus Improved Stochastic and Deterministic Parameterizations. *Journal of Climate*, **25 (14)**, 4946–4962, doi:10.1175/JCLI-D-11-00297.1.

Crimmins, A. R., M. Walsh, and D. Barrie, 2023: Fifth National Climate Assessment. Tech. rep., U.S. Global Change Research Program, Washington, DC, 1834 pp. URL https://nca5.climate.us/.

Durre, I., M. J. Menne, B. E. Gleason, T. G. Houston, and R. S. Vose, 2010: Comprehensive Automated Quality Assurance of Daily Surface Observations. *Journal of Applied Meteorology and Climatology*, **49 (8)**, 1615–1633, doi:10.1175/2010JAMC2375.1.

Durre, I., M. J. Menne, and R. S. Vose, 2008: Strategies for Evaluating Quality Assurance Procedures. *Journal of Applied Meteorology and Climatology*, **47 (6)**, 1785–1791, doi:10.1175/2007JAMC1706.1.

Frassoni, A., and Coauthors, 2023: Systematic Errors in Weather and Climate Models: Challenges and Opportunities in Complex Coupled Modeling Systems. *Bulletin of the American Meteorological Society*, **104 (9)**, E1687–E1693, doi:10.1175/BAMS-D-23-0102.1.

Intergovernmental Panel on Climate Change (IPCC), 2014: Climate Change 2014: Synthesis Report. Contribution of Working Groups I, II and III to the Fifth Assessment Report of the Intergovernmental Panel on Climate Change. Tech. rep., IPCC, Geneva, Switzerland, 151 pp. URL https://www.ipcc.ch/report/ar5/syr/.

Intergovernmental Panel on Climate Change (IPCC), 2023: *Climate Change 2022 – Impacts, Adaptation and Vulnerability: Working Group II Contribution to the Sixth Assessment Report of the Intergovernmental Panel on Climate Change*. Cambridge University Press, Cambridge, doi:10.1017/9781009325844, URL https://www.cambridge.org/core/books/climate-change-2022-impacts-adaptation-and-vulnerability/161F238F406D530891AAAE1FC76651BD.

Kim, G., J. Kim, and D.-H. Cha, 2022: Added value of high-resolution regional climate model in simulating precipitation based on the changes in kinetic energy. *Geoscience Letters*, **9 (1)**, 38, doi:10.1186/s40562-022-00247-6.

Maraun, D., and M. Widmann, 2015: The representation of location by a regional climate model in complex terrain. *Hydrology and Earth System Sciences*, **19 (8)**, 3449–3456, doi:10.5194/hess-19-3449-2015.

Menne, M. J., I. Durre, R. S. Vose, B. E. Gleason, and T. G. Houston, 2012: An Overview of the Global Historical Climatology Network-Daily Database. *Journal of Atmospheric and Oceanic Technology*, **29 (7)**, 897–910, doi:10.1175/JTECH-D-11-00103.1.

Parker, W. S., 2016: Reanalyses and Observations: What's the Difference? *Bulletin of the American Meteorological Society*, **97 (9)**, 1565–1572, doi:10.1175/BAMS-D-14-00226.1.

Pierce, D. W., D. R. Cayan, and B. L. Thrasher, 2014: Statistical Downscaling Using Localized Constructed Analogs (LOCA). *Journal of Hydrometeorology*, **15 (6)**, 2558–2585, doi:10.1175/JHM-D-14-0082.1.

Pierce, D. W., J. F. Kalansky, and D. R. Cayan, 2018: Climate, drought, and sea level rise scenarios for California's fourth climate change assessment. Tech. Rep. CCCA4-CEC-2018-006, California Energy Commission and California Natural Resources Agency, 71 pp.

Stevens, B., and Coauthors, 2020: The Added Value of Large-eddy and Storm-resolving Models for Simulating Clouds and Precipitation. *Journal of the Meteorological Society of Japan. Ser. II*, **98 (2)**, 395–435, doi:10.2151/jmsj.2020-021.

Sugg, M. M., C. E. Konrad, and C. M. Fuhrmann, 2016: Relationships between maximum temperature and heat-related illness across north carolina, usa. *Int J Biometeorol*, **60**, 663–675, doi:10.1007/s00484-015-1060-4.

Zhang, S., Z. Zhou, P. Peng, and C. Xu, 2023: A New Framework for Estimating and Decomposing the Uncertainty of Climate Projections. *Journal of Climate*, **37 (2)**, 365–384, doi:10.1175/JCLI-D-23-0064.1.